

Numerical analysis of radiant warmer

Marek Rojczyk, Ireneusz Szczygieł

Institute of Thermal Technology, Silesian University of Technology

Konarskiego 22, 44-100 Gliwice, Poland

e-mail: marek.rojczyk@polsl.pl

The main objective of this paper is to recognise the heat transfer phenomena between an infant placed in a radiant warmer and the surrounding environment. The influence of the parameters in the computational time during different physical phenomena in heat transfer is studied. This model can be also used in future work to improve radiant warmer efficiency. A complete 2D and 3D numerical simulation was carried out using commercial code ANSYS Workbench – ANSYS Fluent. The analysis involved the fluid flow, convection and radiation heat transfer as well as turbulence modeling, although moisture phenomena were omitted. The experiments were completed to validate a numerical solution.

Keywords: numerical analysis, radiant warmer, radiation, premature infant, CFD, heat transfer, fluid mechanics.

1. INTRODUCTION

In recent years medicine has been developing very quickly. Cases, which were incurable in the past, can be easily treated nowadays. During pregnancy period more women are monitored much more closely, and doctors can even perform surgery inside the placenta. Unfortunately, however, due to environmental pollution, the increasing age of pregnancy amongst women, stimulants (alcohol and drugs), Body Mass Index (BMI) below 19.5, and a working week of more than 40 hours means that the numbers of premature deliveries over the last few years remain in the same 10% range [13, 17–19].

According to the World Health Organization (WHO), a premature infant is a baby who was born between the 22nd and 37th week of pregnancy. The highest possibility for survival and healthy growth is for babies who were born after the 28th week of pregnancy. Before this date they have either the highest mortality rate or they are at risk for numerous medical problems. Younger babies, born before 22nd week of pregnancy are not capable of surviving outside the placenta.

Premature infants are weaker than children which are born after the standard pregnancy period. Their organs are not well developed, so they have problems with breathing and, most importantly, they cannot maintain a constant body temperature [14].

However, the time of birth is not the only parameter for survival; birth weight is another key factor, as it helps to determine if the newborn has the probability of survival and a chance of quick recovery. Chiswick divided birth weight into four categories. Table 1 shows those categories [4–6].

If the body temperature of a newborn, whose weight is less than 1500 grams, decreases even by 1–2°C, the consequences can be very dangerous. Result of this is lethargy in the newborn, and furthermore weak muscular tension and difficulties with breathing may develop. There is a possibility of rapid change within the infant's metabolism, which can lead to massive internal bleeding, and ultimately death.

The biggest problem in neonatology is keeping premature infants alive. But this is not the only challenge faced by healthcare workers. A high level of importance is placed on regular checkups of the infant between the ages of two and six.

Table 1. Birth weight categories [13].

Category	Birth-weight (grams)
Low Birth Weight (LBW)	< 2500
Very Low Birth Weight (VLBW)	< 1500
Extremely Low Birth Weight (ELBW)	< 1000
Incredibly Low Birth Weight (ILBW)	< 800

As mentioned above, the healthy growth of premature infants is a long process which does not finish after leaving the hospital. Undoubtedly, however, better treatment at the time of delivery gives the infants a bigger chance to be in the same condition as healthy children.

Therefore, thanks to a huge amount of research and the creation of incubators, there is a better chance of survival for those children. First type of rescue devices are incubators: closed and open. The second one is known as a radiant warmer.

Generally, the best solution is to place the baby in a closed incubator and to guarantee the optimal thermal conditions for the newborn's further development. Closed incubators protect children from sound and light, and can create conditions with the proper temperature and humidity. However, sometimes the most important thing is to have an easy access to infants during, for example, surgery, so an open incubator (radiant warmer) should be used [23–26, 28–30, 32–36].

2. ENERGY BALANCE OF AN INFANT

2.1. Heat balance equation

The normal human temperature varies with the place of the measurement. In other words, different parts of the body have different temperatures. In the stomach a temperature of 36.2–37.2°C is recorded, and in the core body, measured in the rectum, a temperature of 36.5–37.5°C can be noticed. This is the effect of energy balance: heat generation and loss into the environment. The heat balance equation is presented by American Society of Heating, Refrigerating and Air-Conditioning Engineers (ASHRAE) [1, 6]:

$$M - W = Q_{sk} + Q_{res} = (C_{sk} + R_{sk} + E_{sw} + E_{dif}) + (C_{res} + E_{res}),$$

where M is the metabolic energy production (W m^{-2}), W is the mechanical work (W m^{-2}), Q_{sk} is the skin heat loss (W m^{-2}), Q_{res} is the heat loss through respiration (W m^{-2}), C_{sk} is the convective skin heat loss (W m^{-2}), R_{sk} is the radiative skin heat loss (W m^{-2}), E_{sw} is the evaporative skin heat loss (through sweating) (W m^{-2}), E_{dif} is the evaporative skin heat loss (through moisture diffusion) (W m^{-2}), C_{res} is the convective heat loss from respiration (W m^{-2}) and E_{res} is the rate of evaporate heat loss from respiration (W m^{-2}).

In a healthy person, equilibrium is achieved by heat loss and heat production in the same quantities. Unfortunately, premature infants do not have a developed thermoregulation system, so without protection we cannot assure a constant temperature. More information regarding this will be provided in the following section.

2.2. Infant thermoregulation

Premature infants born before the 32nd week with a very low birth weight (< 1500 gram) have a handicapped thermoregulation system, so they cannot maintain a constant temperature for longer than short periods of time, as in a case of older children and adults. Foetuses exchange 85% of heat through the placenta and only 15% through the skin. The skin of the premature infant is thin and not well developed; thus, heat is lost more rapidly when compared to a full-term baby.

Therefore after delivery, a neutral environment should be ensured with a neutral temperature depending on the body weight and birth time of each individual infant.

Generally, even low fluctuation (even about 1°C) of core body temperature can be dangerous for an infant's life. Consequently, closed incubators and a radiant warmer are absolutely essential [6].

The conclusion is that the temperature of a premature baby strongly depends on environmental conditions [8–11].

2.3. External supporting of thermoregulation system

The first closed incubator (Fig. 1), which worked in the same way as modern apparatus, was constructed in 1880 by Tarnier, and used in the Maternity Hospital of Paris in 1881 [1, 25]. Tarnier constructed the incubator together with Odile Martin, the director of the Paris Zoo, based upon devices that were in use for a long time in chicken farms. Those incubators were able to contain several children; unfortunately, in those days people did not know about the threatening aspects of cross infections, which are the cause of death among many children.

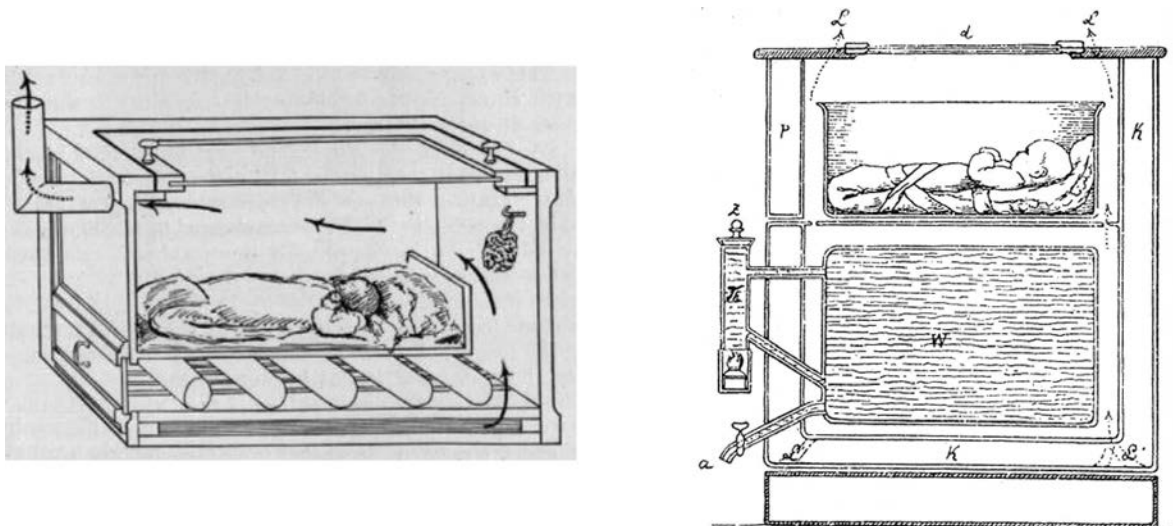


Fig. 1. The Tarnier incubator [5, 16].

The Tarnier incubator controls both temperature and humidity. The water (w , Fig. 1) is heated by the oil flame (π) in the lower chamber, next it evaporates and the warmed air circulates in the upper box guaranteeing that the infant has the proper conditions [5, 16].

Thanks to these simple apparatuses, a huge decrease in infant mortality (for babies weighing less than 2000 grams) from 66% to 38% was achieved [3]. This was a great success, because in those times even healthy children born after the gestation period faced difficulties, and children born before the normal time had small chances to survive [2–4, 7]. Moll has constructed the first machine which generated heat for the baby by using a shining light bulb (Fig. 2). In this case, the infrared phenomenon was used, but its main aim was to cure children with lung disease. The first contemporary incubator which used infrared waves was designed by Agate and Silverman in the 1950s. [3, 25].

Nowadays, thanks to the advancements of technological medicine, more developed constructions have appeared. An incubator not only ensures the proper environmental surroundings, but also monitors and supports survival activities, if necessary. Together with the standardised regulations, they give an increased chance of survival for very immature infants.

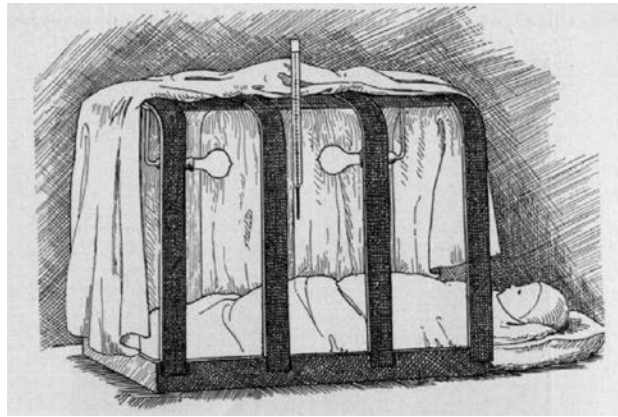


Fig. 2. Moll incubator [5].



Fig. 3. Different types of the radiant warmer: 1 – lamp with infrared bulb, 2 – bed with an insulation or heating mattress.

3. GOVERNING EQUATIONS

The following governing equations were considered: mass conservation equation, momentum conservation equation, energy conservation equation, turbulence equation, radiation equation.

Mass conservation equation

Mass conservation equation is based on a mass balance theory, which states that “the rate of increase of mass in a fluid element is equal to the net rate of flow of mass into the fluid element” and is described in the following equation:

$$\frac{\partial \rho}{\partial t} + \nabla (\rho \mathbf{u}) = 0, \quad (1)$$

where ρ is the density (kg/m^3), ∇ is the nabla operator, t is the time (s), \mathbf{u} is the velocity vector (m/s).

Momentum conservation equation

Newton's second law states that "the rate of increase in the momentum of fluid particles is equal to the sum of forces on fluid particles". In a Newtonian fluid, the viscous stresses are proportional to the rates of deformation. The Navier-Stokes equation is the momentum conservation equation and can be written as follows [27, 31]:

$$\rho \frac{Du}{Dt} = \frac{\partial(-p + \tau_{xx})}{\partial x} + \frac{\partial\tau_{yx}}{\partial y} + \frac{\partial\tau_{zx}}{\partial z} + S_{Mx}, \quad (2)$$

$$\rho \frac{Dv}{Dt} = \frac{\partial\tau_{xy}}{\partial x} + \frac{\partial(-p + \tau_{yy})}{\partial y} + \frac{\partial\tau_{zy}}{\partial z} + S_{My}, \quad (3)$$

$$\rho \frac{Dw}{Dt} = \frac{\partial\tau_{xz}}{\partial x} + \frac{\partial\tau_{yz}}{\partial y} + \frac{\partial(-p + \tau_{zz})}{\partial z} + S_{Mz}, \quad (4)$$

where u , v , w are velocity vectors (m/s), p is the pressure (N/m²), τ is the viscous stress tensor and S_{Mx} , S_{My} , S_{Mz} are source terms.

Energy conservation equation

Energy equation is derived from the **first law of thermodynamics** which states that the rate of change of energy of a fluid particle is equal to the rate of heat addition to the fluid particle plus the rate of work done on the particle.

$$\rho \frac{DE}{Dt} = -\text{div}(p\mathbf{u}) + \left[\frac{\partial(u\tau_{xx})}{\partial x} + \frac{\partial(u\tau_{xx})}{\partial x} + \frac{\partial(u\tau_{xx})}{\partial x} + \frac{\partial(u\tau_{xx})}{\partial x} \frac{\partial(u\tau_{xx})}{\partial x} + \frac{\partial(u\tau_{xx})}{\partial x} \right. \\ \left. + \frac{\partial(u\tau_{xx})}{\partial x} + \frac{\partial(u\tau_{xx})}{\partial x} + \frac{\partial(u\tau_{xx})}{\partial x} + \frac{\partial(u\tau_{xx})}{\partial x} \right] + \text{div}(k \text{grad } T) + S_E, \quad (5)$$

where $E = i + \frac{1}{2}(u^2 + v^2 + w^2)$, i is an internal energy, T is a temperature (K) and S_E is the source term.

Turbulence equations for the RNG k - ε model

The RNG-based k - ε turbulence model is derived from the instantaneous Navier-Stokes equations, using a mathematical technique called the "renormalization group" (RNG) method. The analytical derivation results in a model with constants different to those in the standard k - ε model, and additional terms and functions in the transport equations for k or ε [12, 21, 36].

$$\frac{\partial(\rho k)}{\partial t} + \text{div}(\rho k \mathbf{U}) = \text{div}[\alpha_k \mu_{eff} \text{grad } k] + 2\mu_t E_{ij} E_{ij} - \rho \varepsilon, \quad (6)$$

$$\frac{\partial(\rho \varepsilon)}{\partial t} + \text{div}(\rho \varepsilon \mathbf{U}) = \text{div}[\alpha_\varepsilon \mu_{eff} \text{grad } \varepsilon] + C_{1\varepsilon}^* \frac{\varepsilon}{k} 2\mu_t E_{ij} E_{ij} - C_{2\varepsilon} \rho \frac{\varepsilon^2}{k}, \quad (7)$$

where $\mu_{eff} = \mu + \mu_t$, $\mu_t = \rho C_\mu \frac{k^2}{\varepsilon}$ with $C_\mu = 0.0845$, $\alpha_k = \alpha_\varepsilon = 1.39$, $C_{1\varepsilon} = 1.42$, $C_{2\varepsilon} = 1.42$ and $C_{1\varepsilon}^* = C_{1\varepsilon} - \frac{\eta(1 - \eta/\eta_0)}{1 + \beta\eta^3}$, $\eta = (2E_{ij} \cdot E_{ij})^1 / 2\frac{k}{\varepsilon}$, $\eta_0 = 4.377$; $\beta = 0.012$, k is turbulent kinetic energy (m²/s²), ε is turbulent dissipation rate (m/s), μ_t is dynamic turbulence viscosity (Pa-s), $\mu_t E_{ij}$ is the rate of deformation and $C_{1\varepsilon}$, $C_{2\varepsilon}$, C_μ , η_0 , β , α_k , α_ε are constant.

Radiation modelling

The discrete ordinates (DO) radiation model solves the radiative transfer equation (RTE) for a finite number of discrete solid angles, each associated with a vector direction \mathbf{s} fixed in the global Cartesian system (xyz) . The DO model solves as many transport equations as there are directions. The solution method is identical to that used for the fluid flow and energy equations. The implementation in Fluent uses a conservative variant of the discrete ordinates model called the finite-volume scheme, and its extension to unstructured meshes [6].

The radiative transfer equation for an absorbing, emitting and scattering medium at position r in the direction s is

$$\nabla (I(\mathbf{r}, \mathbf{s}) \mathbf{s}) + (a + \sigma_s) I(\mathbf{r}, \mathbf{s}) = an^2 \frac{\sigma T^4}{\pi} + \frac{\sigma_s}{4\pi} \int_0^{4\pi} I(\mathbf{r}, \mathbf{s}_s) \Phi(\mathbf{s}, \mathbf{s}_s) d\Omega, \quad (8)$$

where \mathbf{r} is position vector, \mathbf{s} is direction vector, \mathbf{s}_s is scattering direction vector, s is a path length, a is an absorption coefficient, n is reflective index, σ_s is a scattering coefficient (m^{-1}), σ is a Stefan-Boltzmann constant ($5.672 \times 10^{-8} \text{ W m}^{-2} \text{ K}^{-4}$), I is a radiation intensity, which depends on position \mathbf{r} and direction s , T is a local temperature (K), Φ is a phase function and Ω is a solid angle (sr).

4. NUMERICAL MODEL

4.1. Geometry

All dimensions in the geometrical model are taken from the real radiant warmer. The surface of the skin area of the baby was assumed as a typical size for a premature baby. The undertaken values are described in Figs. 4 and 5 and they are presented in Tables 2 and 3.

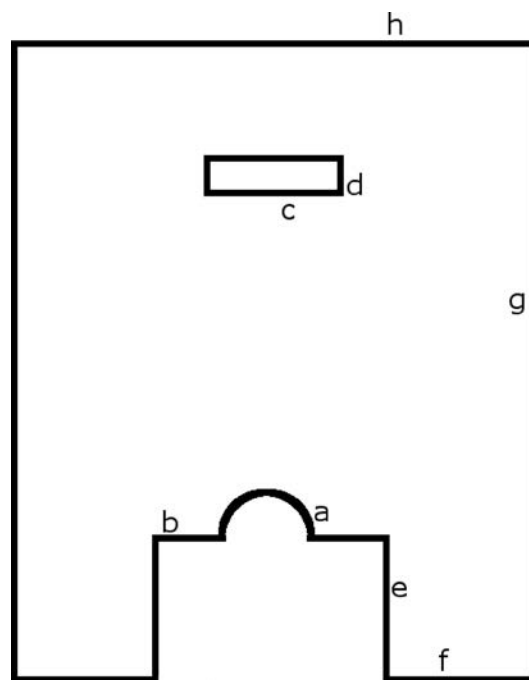


Fig. 4. 2D model.

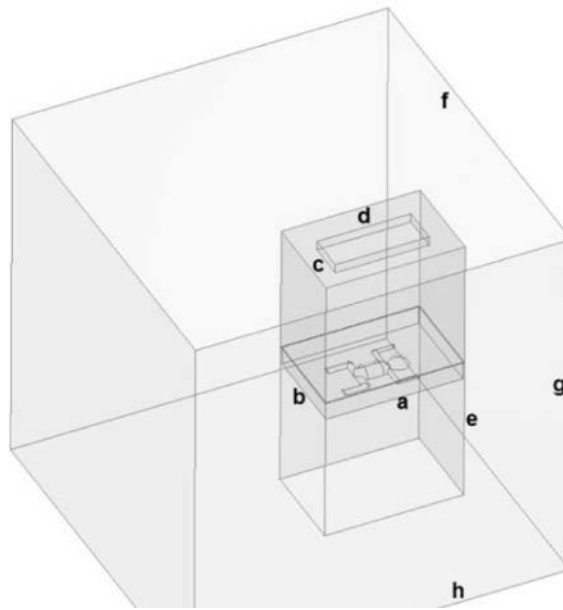


Fig. 5. 3D model.

Table 2. Dimensions in 2D model.

Edge mark	Length [m]
a	0.09 (radius)
b	0.155
c	0.25
d	0.07
e	0.3
f	0.5
g	1.5
h	1.49

Table 3. Dimensions in 3D model.

Edge mark	Length [m]
a	0.74
b	0.49
c	0.2
d	0.5
e	0.5
f	2.0
g	2.0
h	2.0

4.2. Boundary conditions (BC) types

Once the governing equations are defined, boundary and initial conditions must be adequately prescribed in order to complete the problem [20, 22, 37].

Differential energy equation has an infinite number of solutions, and whereas finding these is not a problem, the real problem is to obtain the proper solutions. Therefore, we have to define explicit conditions, of which there are five types:

- geometric conditions (describing shape and body size);
- physical properties (e.g., specific heat, density, thermal conductivity, and their function on the temperature);
- heat sources efficiency;
- initial conditions (describing distribution of the temperature in the whole body at conventional time beginnings, $\tau=0$);
- boundary conditions, describing the conditions of heat transfer on edges (2D) or faces (3D) [15].

In the model, the following types of BCs were used:

Pressure inlet boundary conditions

Pressure inlet boundary conditions are used to define the fluid pressure at flow inlets, along with all other scalar properties of the flow. In incompressible flow, relations between total pressure and the static pressure to the inlet velocity equation were described by Bernoulli in the following:

$$p_0 = p_s + \frac{1}{2}\rho v^2, \quad (9)$$

where v is a velocity (m/s), p_s is a static pressure at the inlet plane (N/m^2) and ρ is a constant density at the inlet plane (kg/m^3).

Pressure outlet boundary conditions

Pressure outlet boundary conditions are used to define the static pressure at flow outlets (and also other scalar variables, in case of backflow). The solver used inlet static pressure and extrapolated all other conditions from the interior of the domain.

Wall boundary conditions

While solving the energy equation, thermal boundary conditions at the wall boundaries have to be defined. There are three different types of possible conditions available:

- temperature boundary conditions;
- heat flux boundary conditions;
- convection boundary conditions.

Temperature boundary condition (Dirichlet)

With the Dirichlet temperature in the wall is assumed as known:

$$T(\bar{\Gamma}) = \bar{T}(\Gamma). \quad (10)$$

Heat flux boundary condition (Neumann)

Neumann heat flux assumes boundary heat flux as known quantify:

$$\dot{q}(\bar{\Gamma}) = \bar{q}(\bar{\Gamma}). \quad (11)$$

Convective boundary condition (Robin)

With convective boundary condition heat flux in the wall is computed using an external heat transfer coefficient and an external heat sink temperature, which is presented below:

$$\dot{q}(\bar{\Gamma}) = h_f (T_w - T_{amb}) + \dot{q}_{r,w}, \quad (12)$$

where h_f is the heat transfer coefficient ($\text{W m}^{-2} \text{K}^{-1}$), T_w is the wall surface temperature (K), $\dot{q}_{r,w}$ is the radiative heat flux from the boundary wall (W m^{-2}), defined as following:

$$\dot{q}_{r,w} = (1 - \varepsilon_{\lambda,w}) \dot{q}_{r,in} + \varepsilon_{\lambda,w} \sigma T^4, \quad (13)$$

where $\dot{q}_{r,in}$ is the incident radiation heat flux (W m^{-2}).

4.3. Boundary conditions applied in 2D and 3D model

Names of boundary conditions are shown in Fig. 6 for 2D and in Fig. 7 for 3D. Boundary conditions' types assumed in the model are presented in Tables 4 and 5.

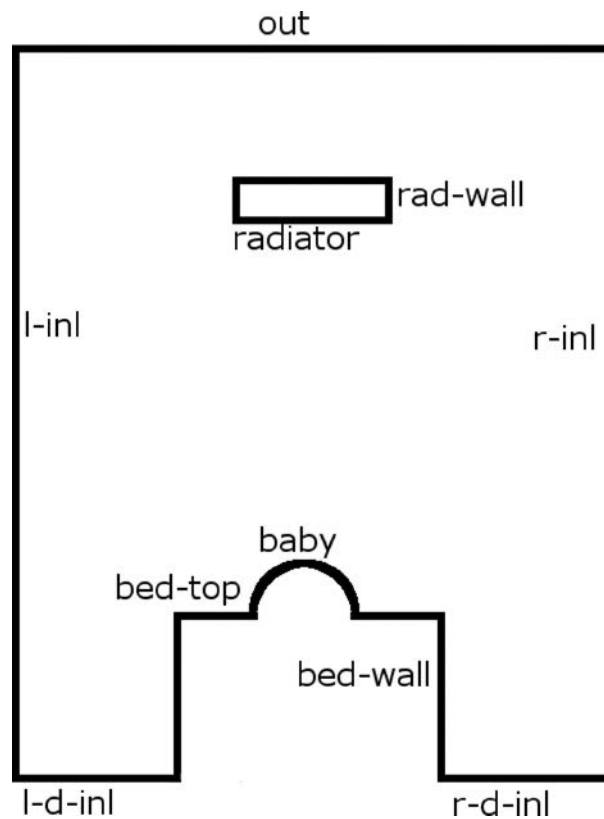


Fig. 6. 2D model.

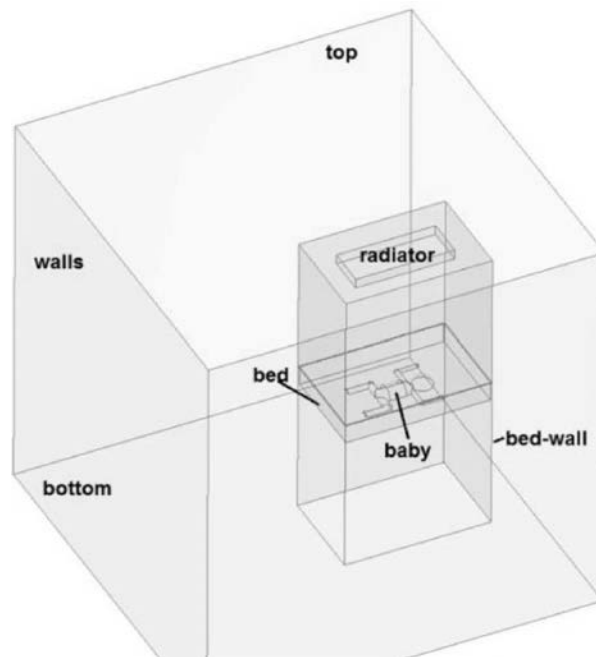


Fig. 7. 3D model.

Table 4. Types of BCs in 2D.

No.	B.C. names	B.C.
1.	baby	Dirichlet
2.	bed-top	Dirichlet
3.	bed-wall	Neumann
4.	radiator	Neumann
5.	rad-wall	Neumann
6.	out	pressure-outlet
7.	l-inl	pressure-inlet
8.	l-d-inl	pressure-inlet
9.	r-inl	pressure-inlet
10.	r-d-inl	pressure-inlet

Table 5. Types of BCs in 3D.

No.	B.C. names	B.C. type
1.	baby	Dirichlet
2.	bed	Neumann
3.	bed-wall	Neumann
4.	radiator	Neumann
5.	top	Dirichlet
6.	bottom	Dirichlet
7.	walls	Dirichlet

4.4. Boundary conditions parameters

The values of the most important parameters of the BCs are presented in Table 6 [15, 22, 27]. Table 6 shows the information about particular elements of the model.

Table 6. Boundary conditions.

Geometry	Face name	Parameter	Value	Unit
2D	baby	Temperature	36.8	°C
		Emissivity	0.95	–
	bed-top	Temperature	36.5	°C
		Emissivity	0.92	–
	radiator	Heat flux	2400	W/m ²
	3D	baby	Temperature	35.0
Emissivity			0.95	–
bed		Heat flux	0	W/m ²
		Emissivity	0.92	–
radiator		Heat flux	6000	W/m ²
top bottom walls		Temperature	20	°C
		Emissivity	0.95	–

4.5. Evaluation of the emissivity

In the radiation calculation an emissivity on the surface body is a very significant parameter. In human skin this parameter is equal to almost one, $\varepsilon = 0.98$. However, the skin of a premature baby is not as developed when compared to an adult.

The emissivity was evaluated by comparing two temperature measurements, using infrared camera and thermocouples, and only proper estimates can result in coherent values of both measurements. The temperatures were taken from eight healthy infant subjects, and two characteristic points located on the infant's body were chosen, one next to the belly button and another one on the leg. After measuring the points' temperature with thermocouples, several infrared pictures with different values of emissivity were taken (Figs. 8–11). On the basis of these results the value of the emissivity was assumed on the level of 0.95. Selected results are presented in Table 7.



Fig. 8. Temperature on a stomach, $\varepsilon = 0.95$.



Fig. 9. Temperature on a stomach, $\varepsilon = 0.98$.

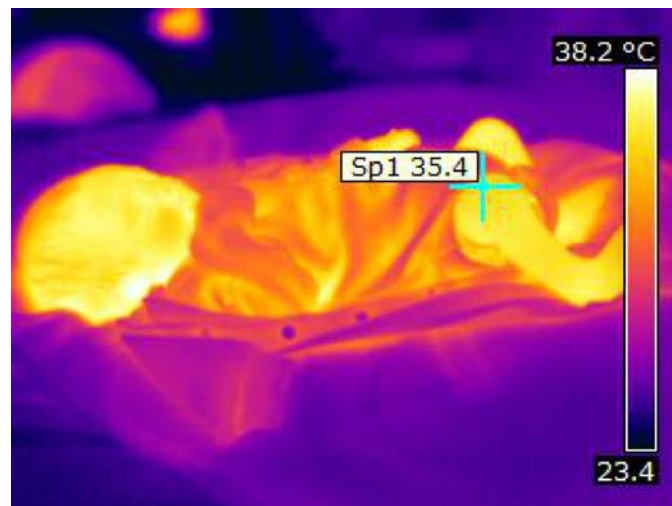


Fig. 10. Temperature on a leg, $\varepsilon = 0.95$.

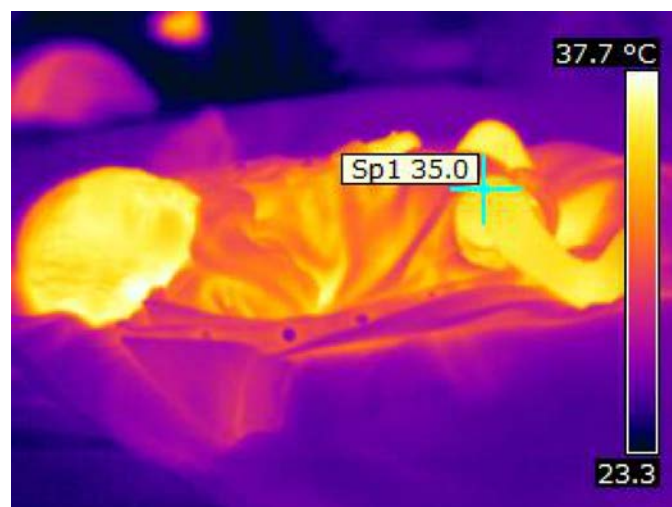


Fig. 11. Temperature on a leg, $\varepsilon = 0.98$.

Table 7. Thermograph and thermocouple temperature measurements.

Case	Thermocouple temperature	Thermograph temperature		Emissivity taken to calculations
		$\epsilon = 0.95$	$\epsilon = 0.98$	
Figs. 8 & 9	36.9	37.0	36.6	$\epsilon = 0.95$
Figs. 10 & 11	35.2	35.4	35.0	

4.6. Mesh in the 2D and 3D model

Grid generation is a domain sub-division of non-overlapping cells, and this process follows further geometry generation. Mesh generation is one of the most complicated processes in a CFD project.

Building the geometry and meshing is the most time-consuming part of the so-called pre-processing. Accuracy of the computations strongly depends on the number of cells, so the larger number of elements is advantageous. A more detailed mesh results in more precise results, but requires much more computations and more powerful computer hardware.

For the sake of the limitations of hardware and time it is very important to find a compromise between the number of cells and solutions accuracy. In practice, this means creating and testing a few meshes with different numbers of elements, what is called a “grid independence test” and choosing the best one, which returns the acceptable results with the smallest number of elements. In the paper, the chosen grid consist of 32 000 triangular elements for 2D and 2.5 million tetrahedrons for 3D. The selected parts of 2D mesh were shown in Figs. 12–14 while 3D mesh parts are presented in Figs. 15 and 16.

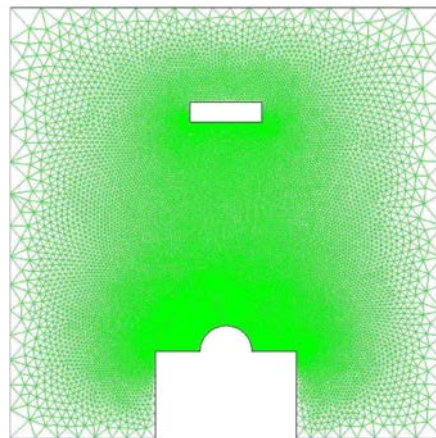


Fig. 12. Mesh heterogeneity.

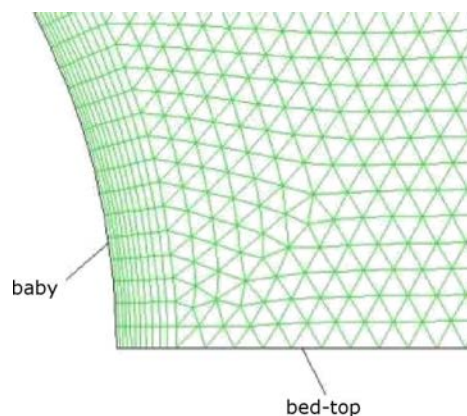


Fig. 13. Cell size next to a baby maintains the same scale as in Fig. 14.

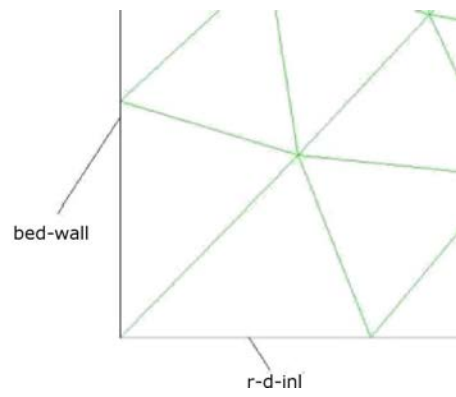


Fig. 14. Cell size next to right-down-inlet maintains the same scale as in Fig. 13.

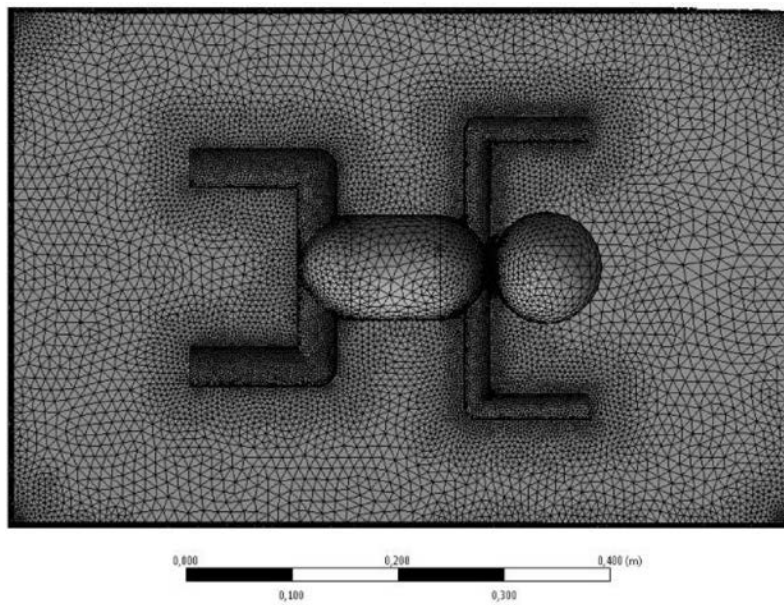


Fig. 15. Cell size on a baby.

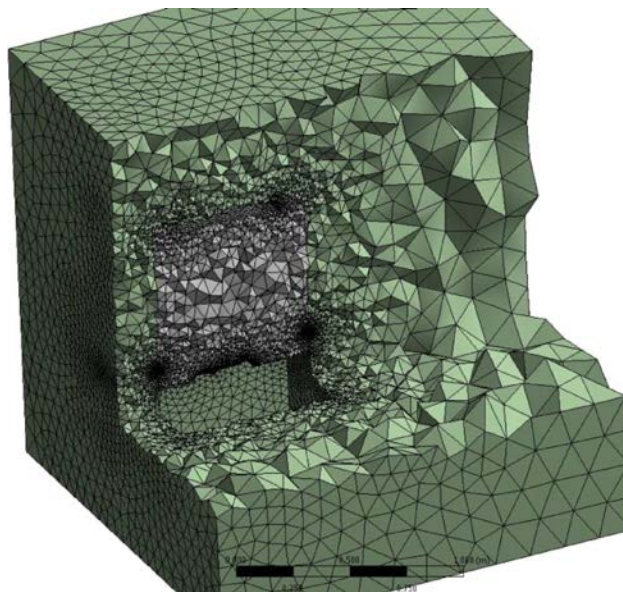


Fig. 16. Differences in cell size in the domain.

5. VALIDATION AND VERIFICATION

The model was computed using ANSYS Fluent. The important part of the numerical modeling process is to check if the model is well-defined. For this reason, a laboratory stand was constructed. In the paper the verification of 2D case is presented.

The laboratory stand was built with a cylinder heater, with installed thermocouples for measuring the temperature on the heater and just above it (Fig. 17). A very characteristic natural convection beak can be noticed both in the experimental measurement as well as in the computational results (Fig. 18 left and right).

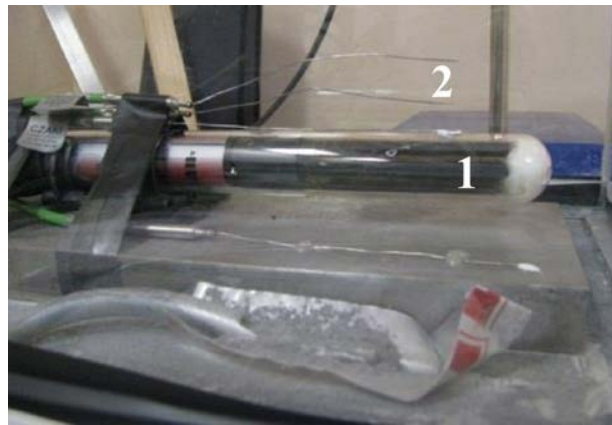


Fig. 17. The model of an infant baby (1) with thermocouples (2).

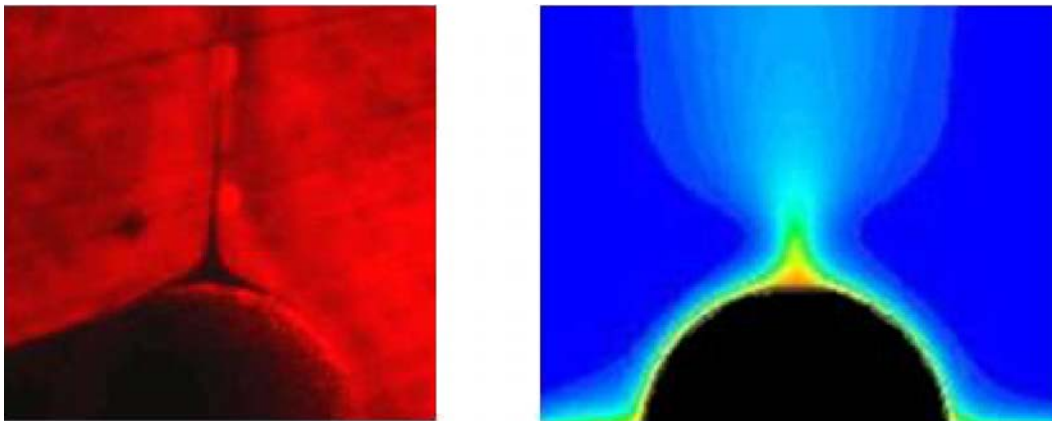


Fig. 18. Flow field above infant model. An experimental solution (left), a numerical solution (right). The shade on the left-hand side of Fig. 18 (left) appears because the laser was on the right-hand side of the model.

The experimental flow field surrounding the heater is shown in Fig. 19. In Fig. 20 a numerical solution is shown next to the baby model. These experiments illustrate that the temperatures are similar on the body surface as well as above it. In both cases, a beak is clearly visible. This beak is characteristic for natural convection. Velocity distribution was measured using PIV method. Temperature is measured by thermocouples. Almost the same values of temperature and velocity are obtained as in the numerical modelling case.

The 3D verification is now under development, the laboratory stand is presented in Fig. 21.

Temperatures in the whole domain with wall temperature were measured. The velocities above the baby model as well as temperatures were measured.

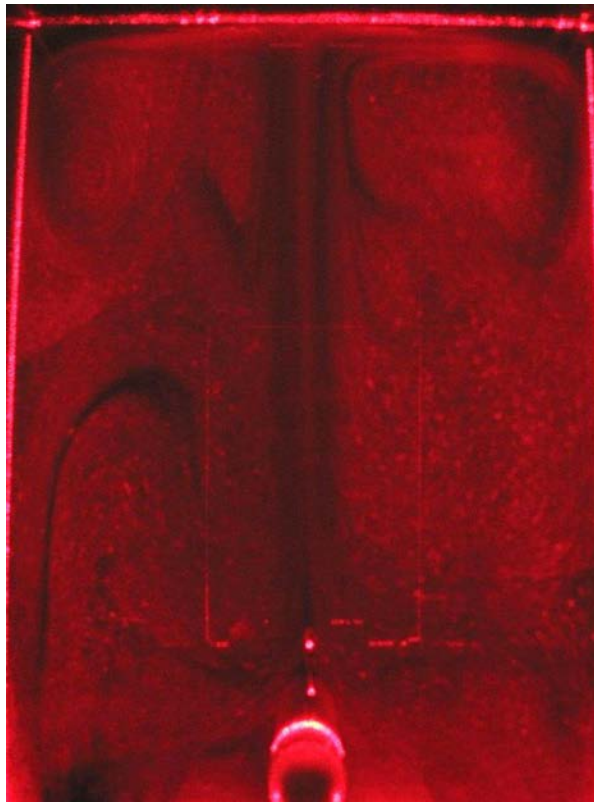


Fig. 19. Velocity vectors during the experiment.

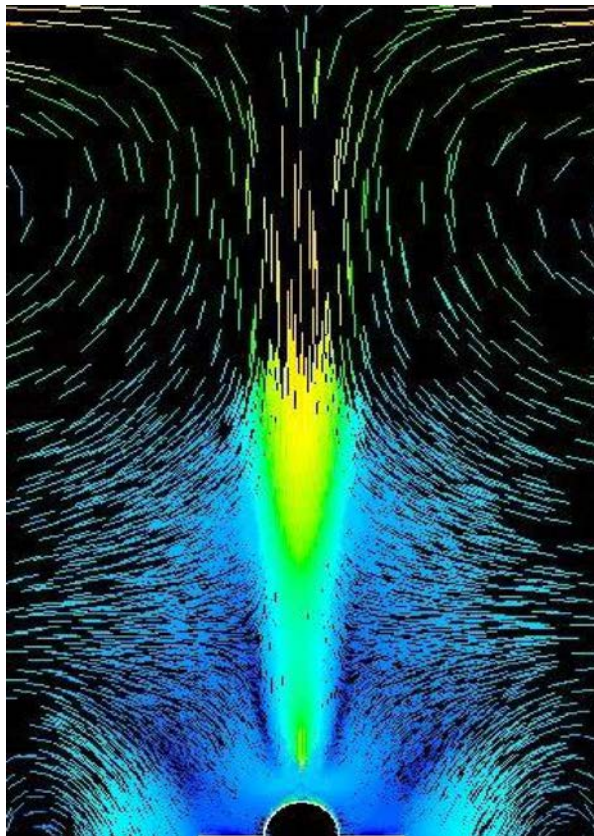


Fig. 20. Velocity vectors in computations.



Fig. 21. 3D verification under development.

6. MULTI-VARIANT ANALYSIS

The main objective of this project is to build and well describe 2D and 3D model of radiant warmer. This model will be used in the future work to optimize functioning of newly designed radiant warmers.

The 2D and 3D models were analysed. The following cases were assumed:

- all processes are considered as a steady-state;
- the fluid as an incompressible ideal gas was admitted;
- the fluid is transparent for radiation;
- air is viscous and analysed by $k-\varepsilon$ RNG (renormalization group) turbulence model;
- radiation is consideration by the discrete ordinate radiation model [15];
- moisture phenomena was omitted.

6.1. 2D model

Several cases of radiant warmer operation were analysed.

Switched off state

In this case the air around the bed is heated up by the body and moves up. Figures 22 and 23 present the contours of the temperature distribution and velocity vectors. The highest temperature

is observed to accumulate next to the semicircle's top, which is an intuitive process. The vectors with highest value of velocity are located on both sides of radiator lamp, as a result of mass conservation.

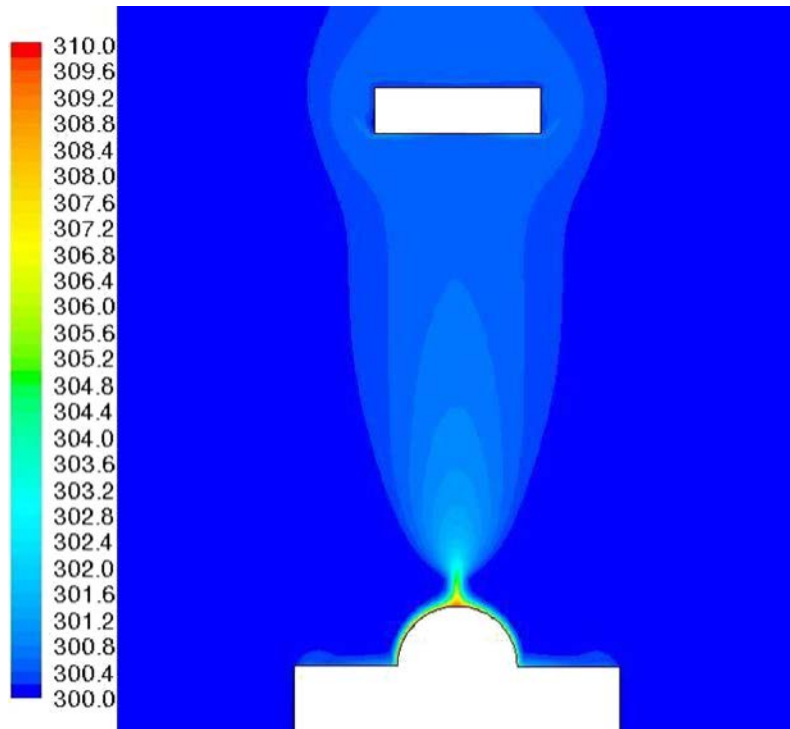


Fig. 22. Contours of the static temperature in the case with natural convection only (K).

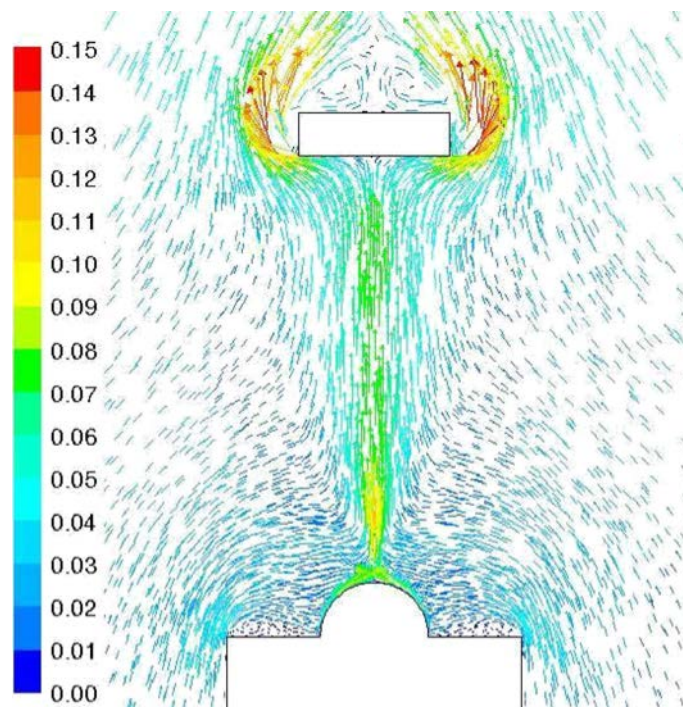


Fig. 23. Velocity vectors coloured by velocity magnitude, plotted in the main area in the case of natural convection only (m/s).

Mattress heating case

In this case, the mattress acts as a heat source. The natural convection is stronger compare to the previous case. Distributions of the temperature and velocity are presented in Figs. 24 and 25.

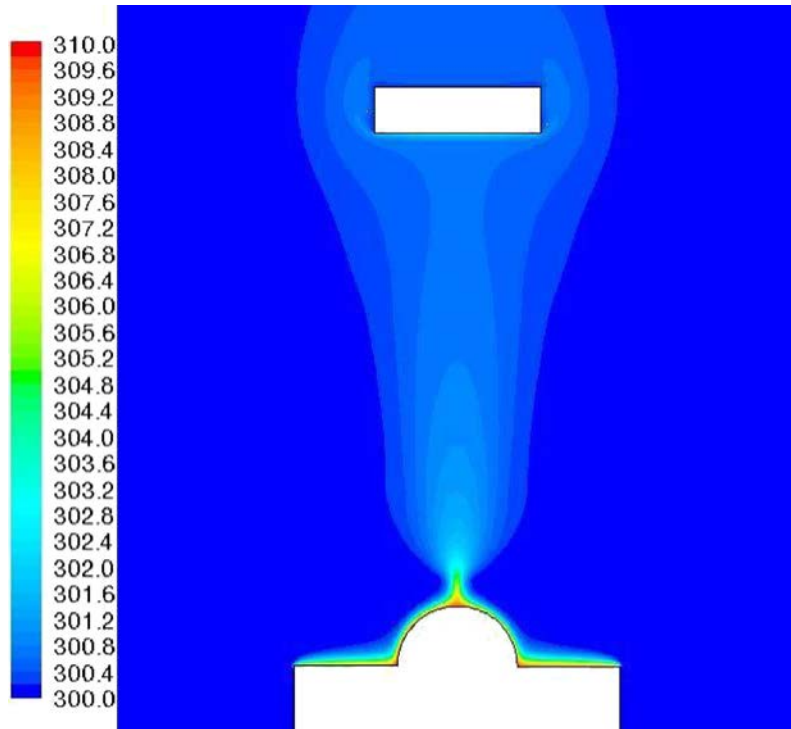


Fig. 24. The contours of static temperature in the case of natural convection only and a mattress switched on (K).

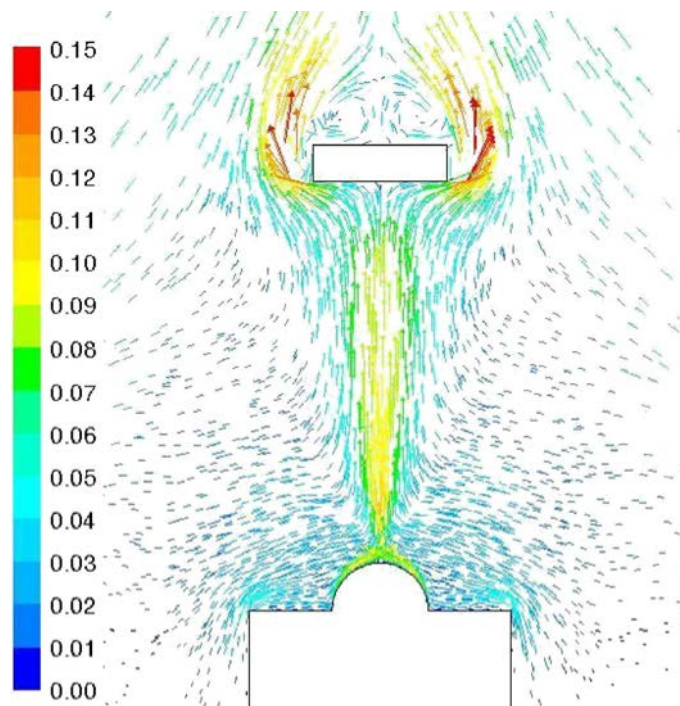


Fig. 25. Velocity vectors coloured by velocity magnitude, plotted in the main area in the case with only natural convection and a mattress switched on (m/s).

Lamp and mattress heating case

In this case, both mattress and lamp work as heat source. Lamp emits the electromagnetic waves in an infra-red spectrum which increases the temperature of all encountered bodies, especially the infant's skin. The operating radiator introduces considerable changes.

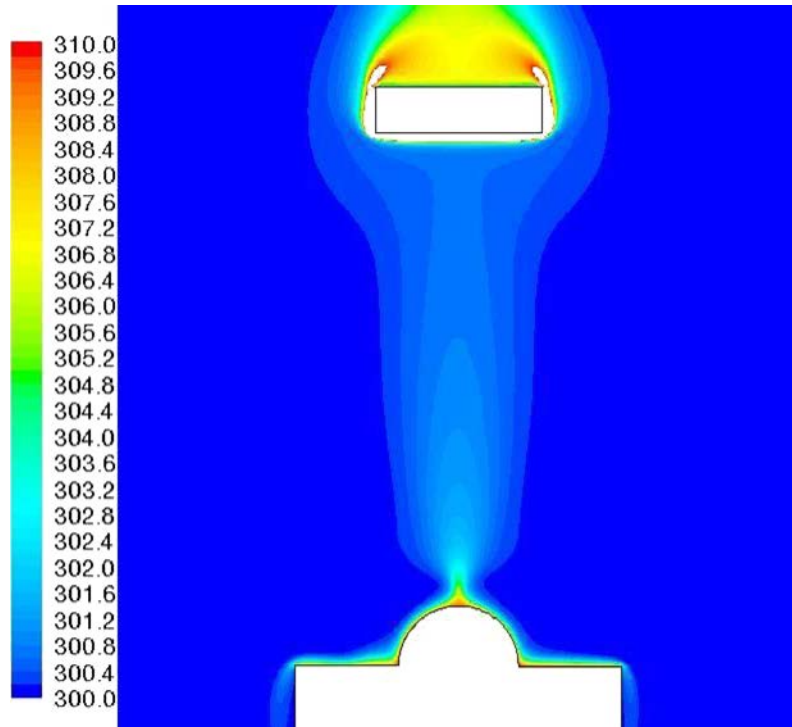


Fig. 26. Contours of static temperature in the case with all conditions-natural convection, switched on mattress and radiation (K).

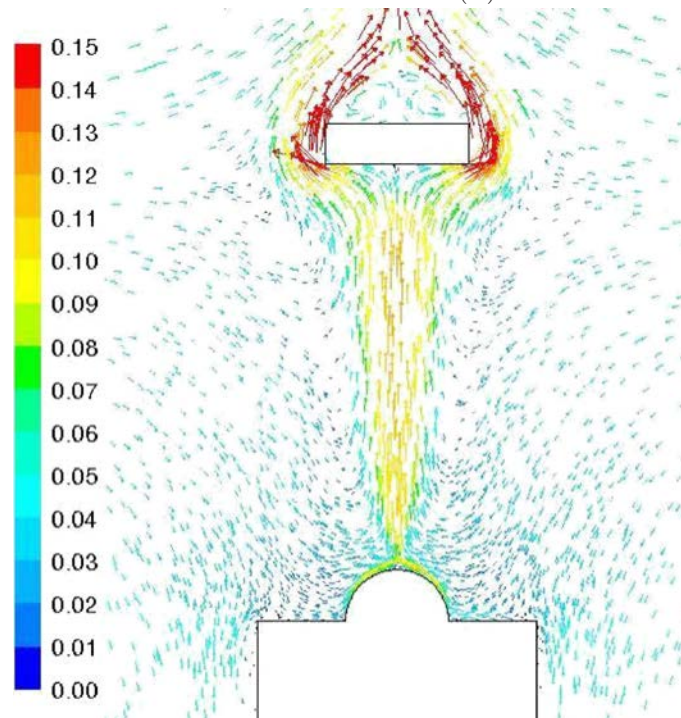


Fig. 27. Velocity vectors coloured by velocity magnitude, plotted in the main area in the case of all conditions-natural convection, switched on mattress and radiation (m/s).

Natural convection chimney is wider and better recognised. More air than in previous case is rising with higher velocities. Distributions of the temperature and velocity are presented in Figs. 26 and 27.

The results presented in the 2D model are comparable with the experiments.

6.2. 3D model

Three cases were analysed:

- switched off state;
- turned on radiator lamp with a half of the available power – 300 W;
- turned on radiator lamp with the full availability of power – 600 W.

In Figs. 30–39, one can observe a temperature fields and velocity vectors in the 3D model present in the cross-section through the child's head and arms and the second cross-section lengthways along the baby.

As it can be observed, the temperature field and velocity vectors have the similar tendencies as in the 2D model.

Switched off case

Figures 28–31 show the temperature fields and velocity vectors, in the case when an infrared lamp is switched off. A loss of heat from the body to the environment can be observed. The air heats up and rises. The shape of temperature distribution is not as regular as in the semicircle in 2D calculations, because the shape of the body is based on a real baby. Velocity vectors and the temperature are in the same range as in the 2D model. The same as in an experiment and in 2D calculations characteristic natural convection beak is visible.

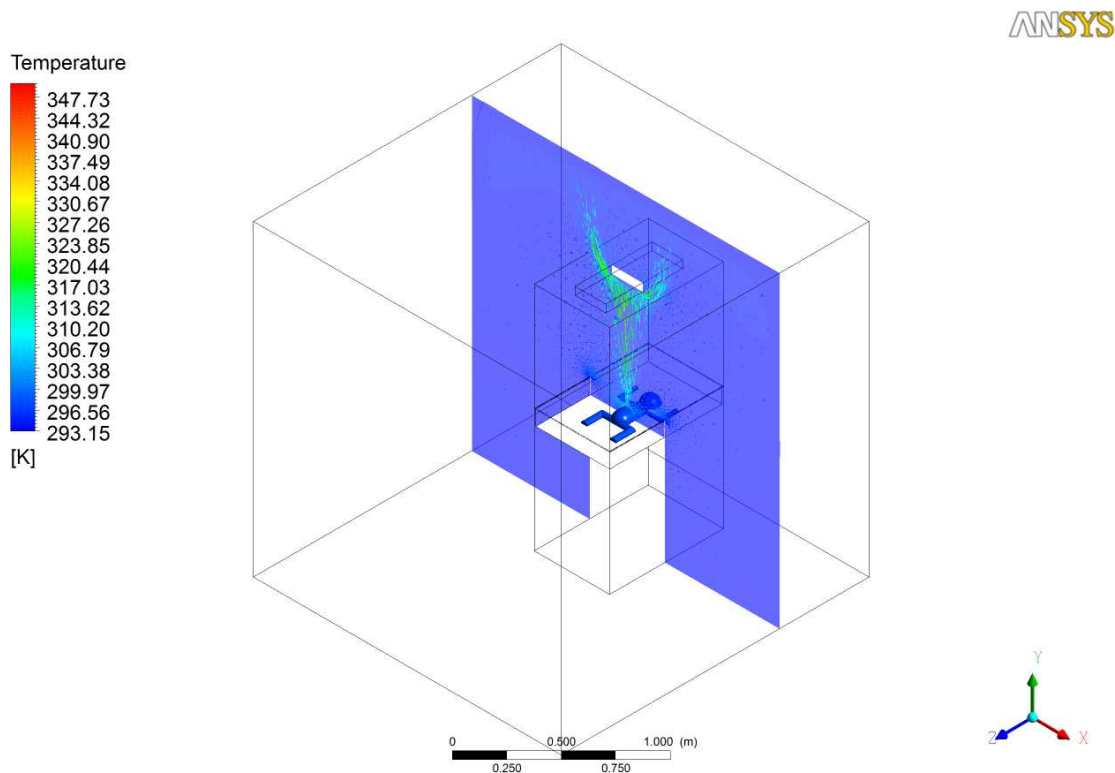


Fig. 28. Temperature and velocity vectors in the case without radiator lamp, general view.

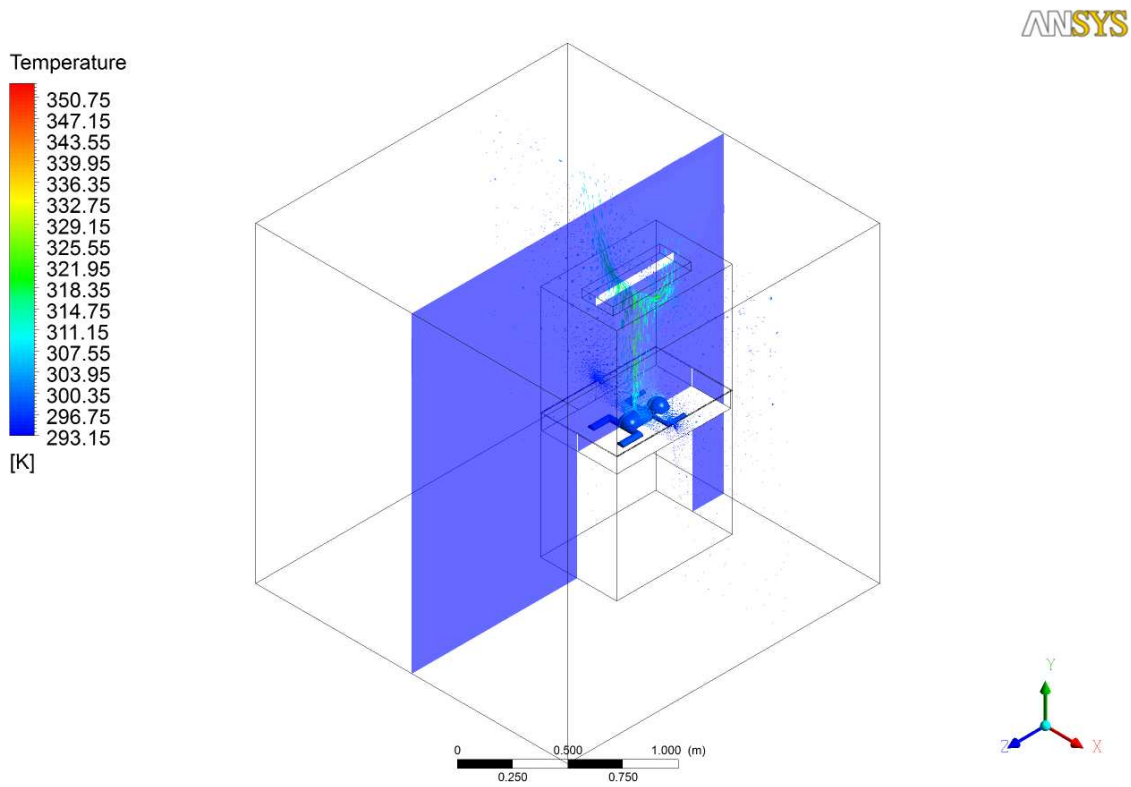


Fig. 29. Temperature and velocity vectors in the case without radiator lamp, general view.

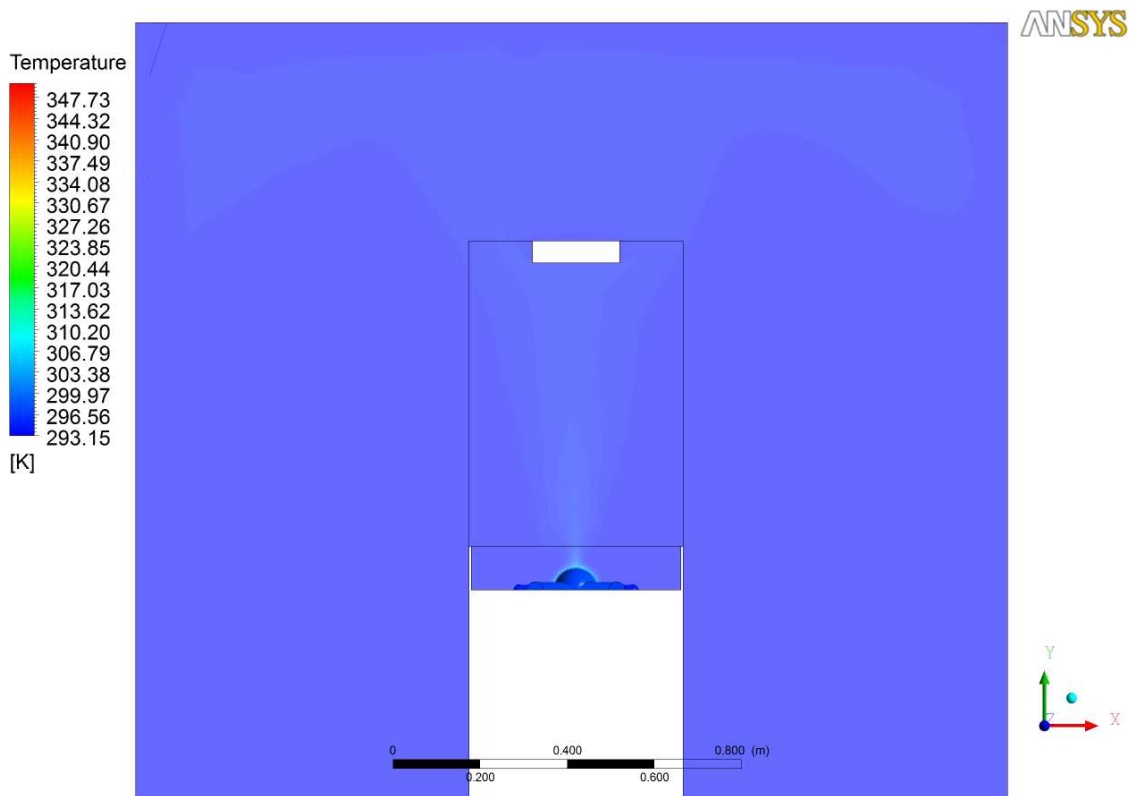


Fig. 30. Temperature in the case without radiator lamp, cross-section view.

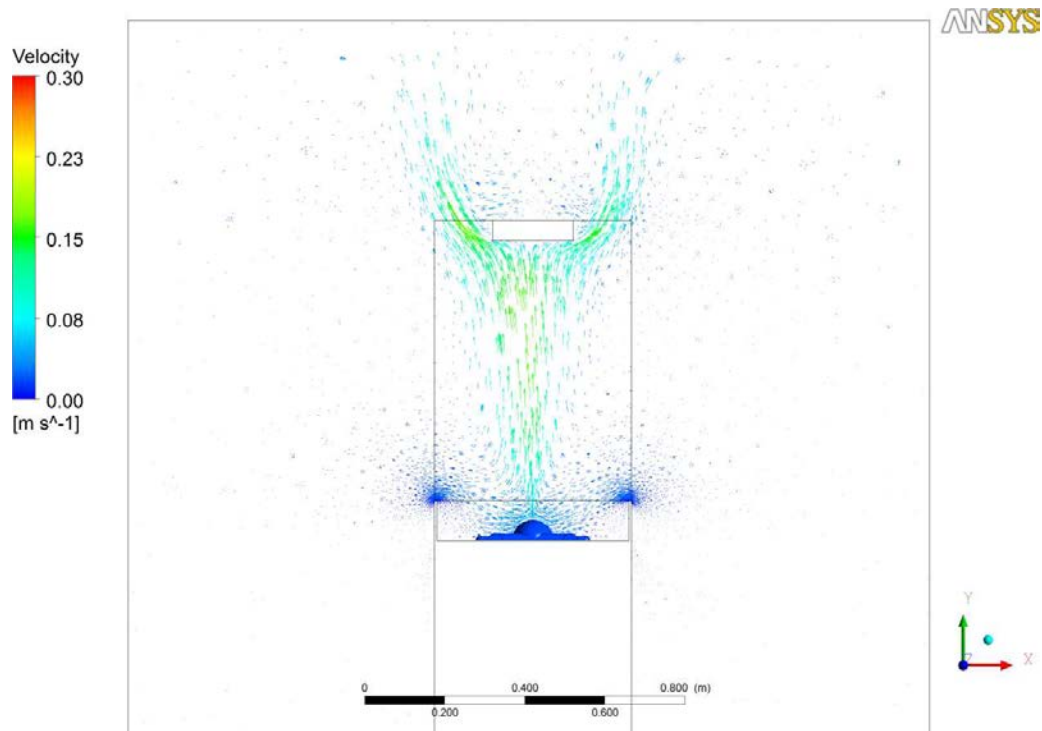


Fig. 31. Velocity vectors in the case without radiator lamp, cross-section view.

Half power radiator lamp case

Figures 32–35 show the temperature fields and velocity vectors in the case when a half of the power of the radiator is assumed. The air heats up and rises with a higher temperature and velocity vectors than in previous case.

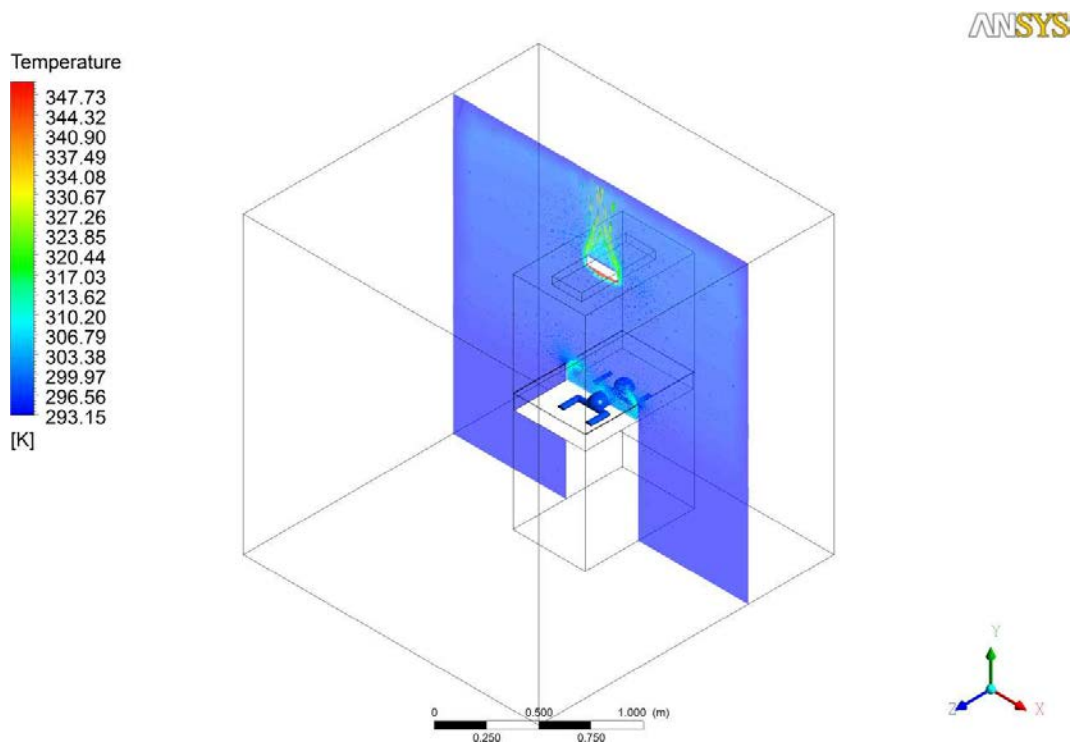


Fig. 32. Temperature and velocity vectors in the case with a 300 W power radiator lamp, general view.

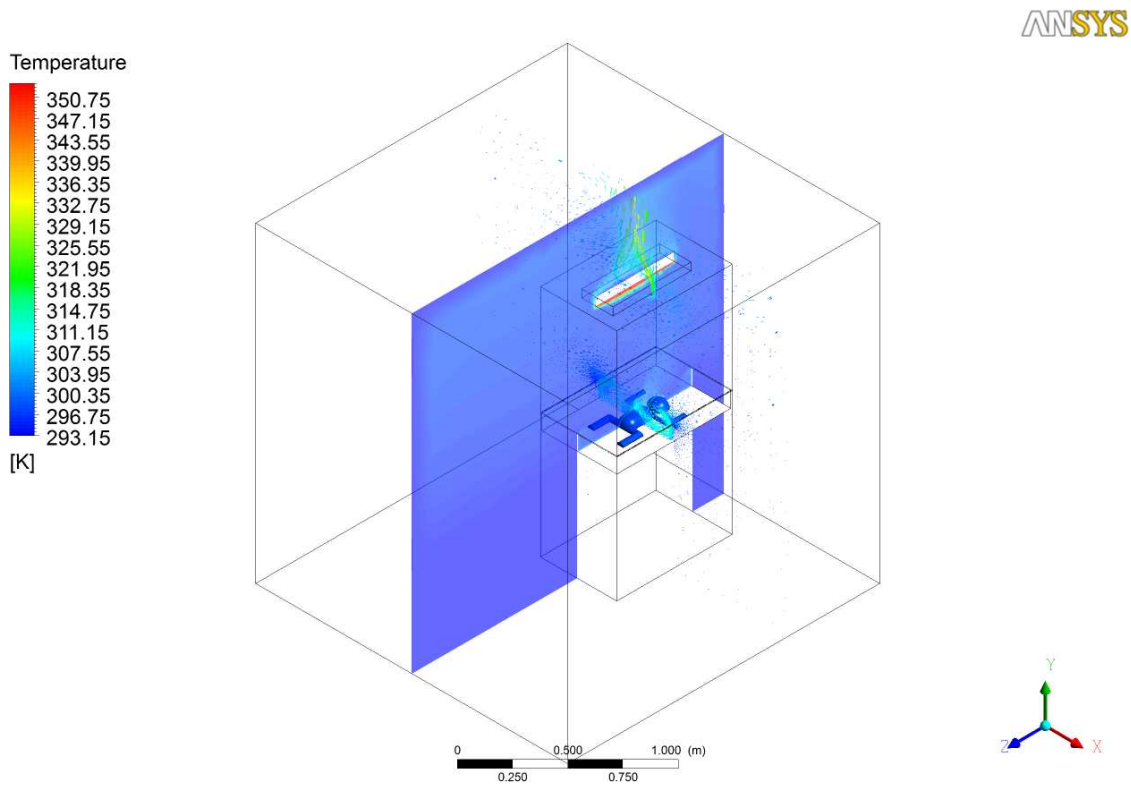


Fig. 33. Temperature and velocity vectors in the case with a 300 W power radiator lamp, general view.

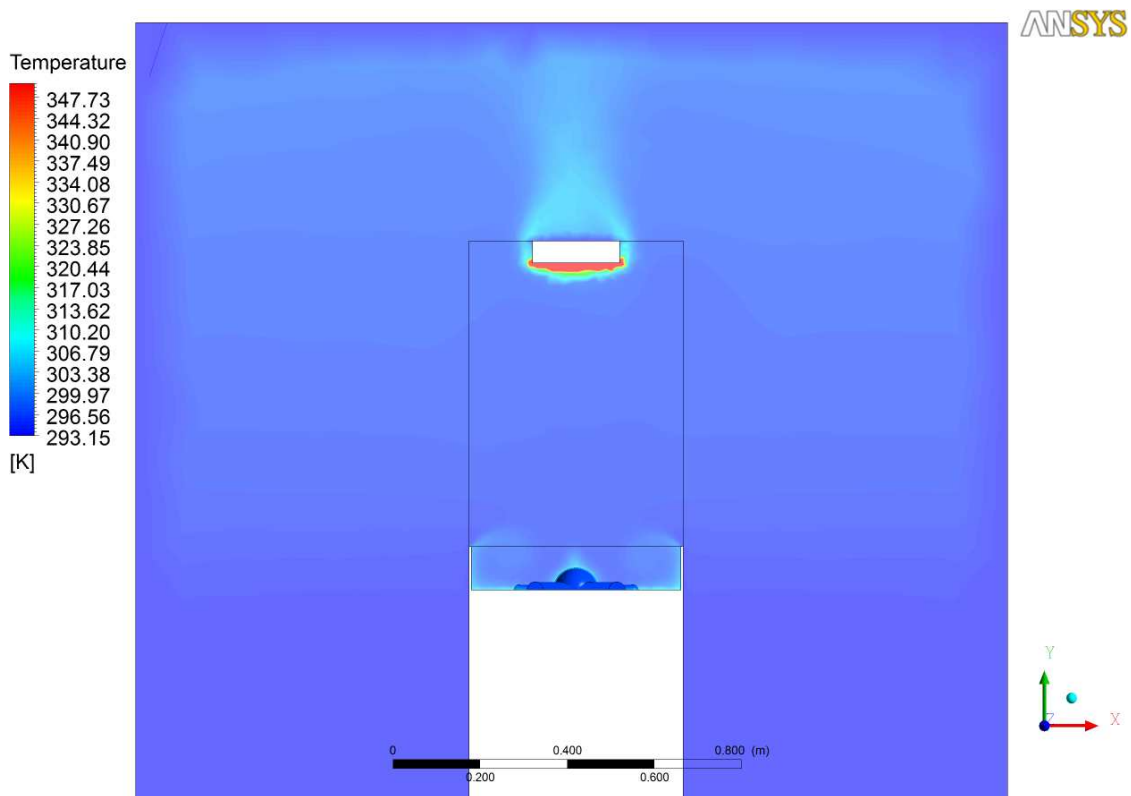


Fig. 34. Temperature in the case with a 300 W power radiator lamp, cross-section view.

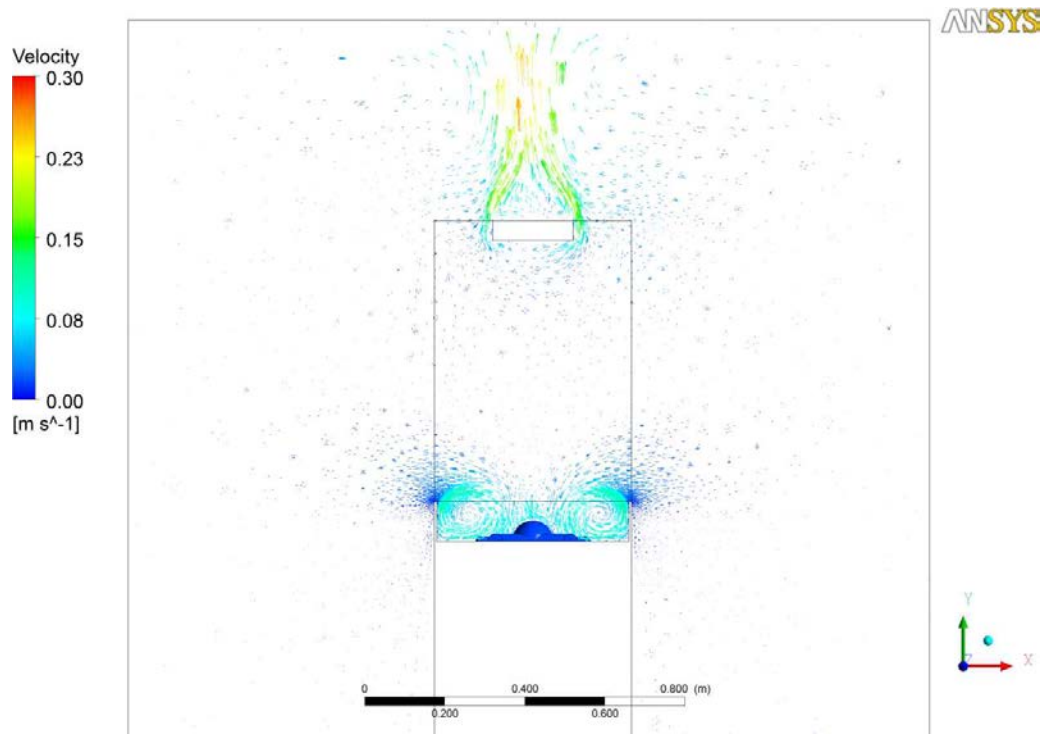


Fig. 35. Velocity vectors in the case with a 300 W power radiator lamp, cross-section view.

Full power radiator lamp case

Figures 36-39 show the temperature fields and velocity vectors in the case with natural convection and radiation. Next to the body, due to the radiator, a higher air temperature can be observed. It

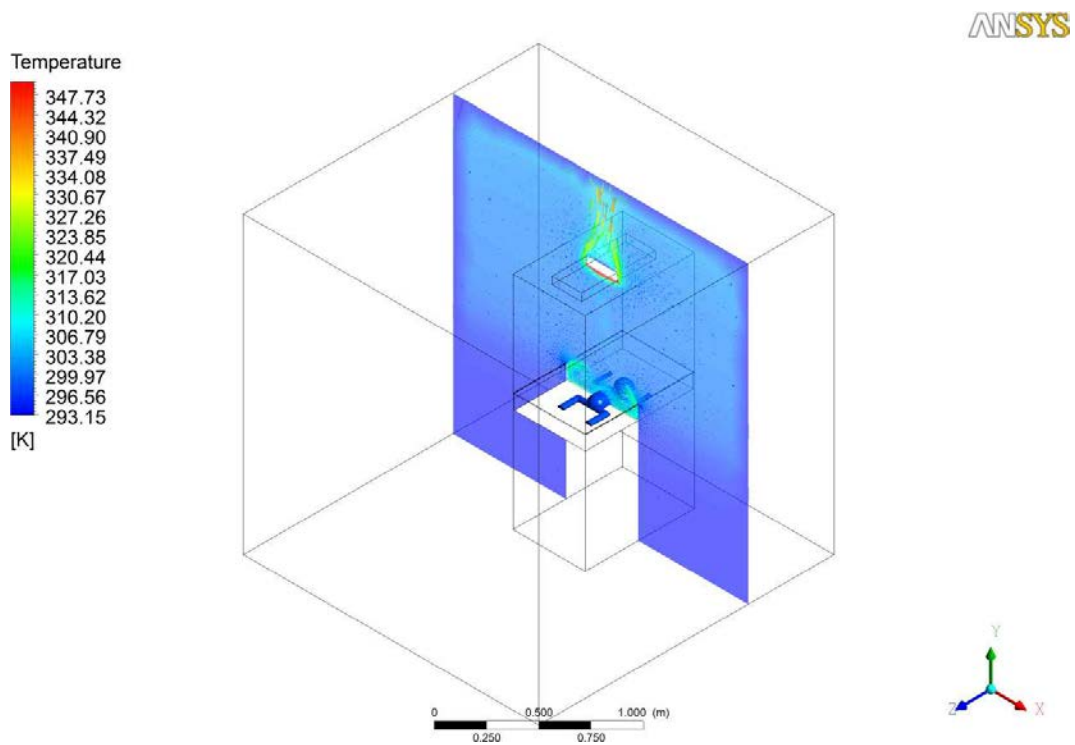


Fig. 36. Temperature and velocity vectors in the case with a 600 W power radiator lamp, general view.

means that the incubator keeps the infant warm. The air is heating up from the body and rising. Velocity vectors have higher values in comparison to the previous results.

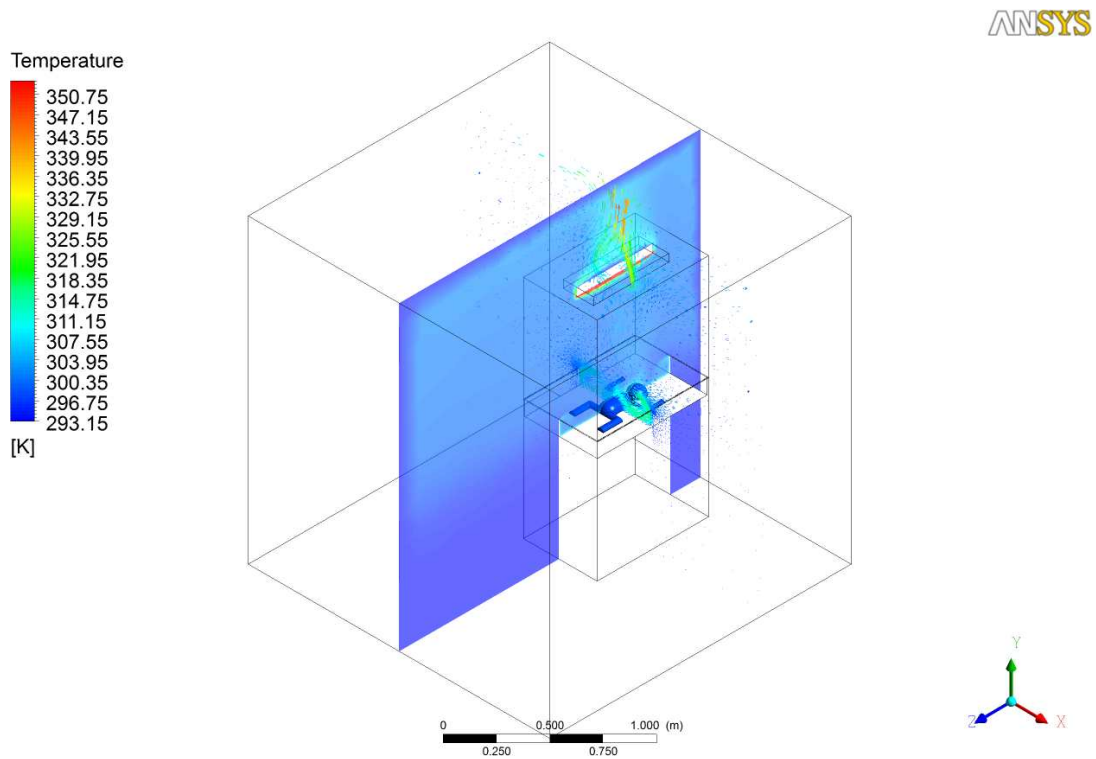


Fig. 37. Temperature and velocity vectors in the case with a 600 W power radiator lamp, general view.

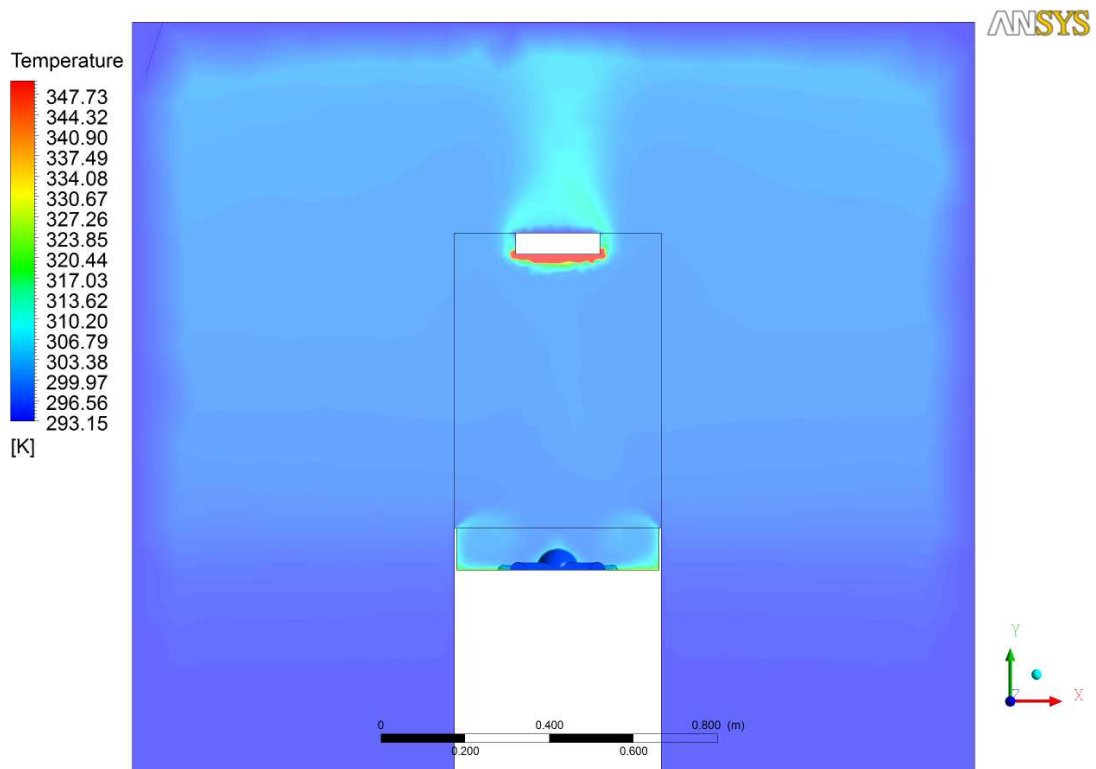


Fig. 38. Temperature in the case with a 600 W power radiator lamp, cross-section view.

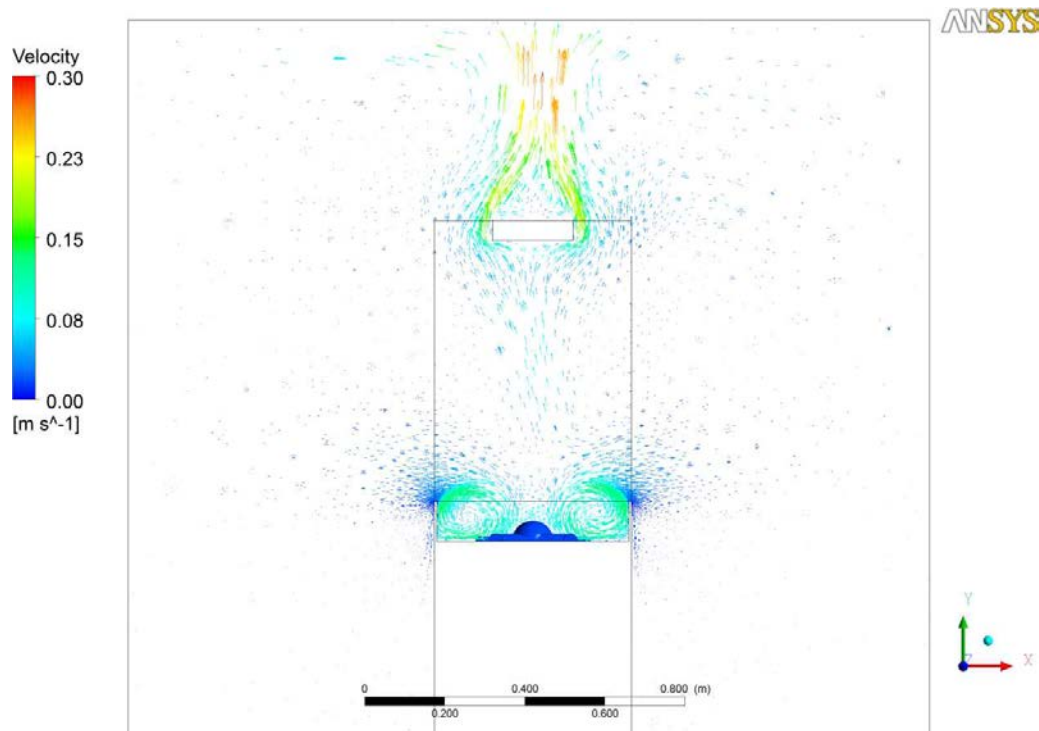


Fig. 39. Velocity vectors in the case with a 600 W power radiator lamp, cross-section view.

In this and other 3D cases, model contains characteristic for a radiant warmer plastic shields, which are located around baby's bed. These shields protect the infant from falling out of bed, and their height prevents unexpected side air flows which could cool the infant. This is a reason why in 3D analysis air flow next to the bed is different than in 2D case. In 3D case, air eddies next to the infant are visible.

7. CONCLUSIONS

A radiant warmer is a very important device in every hospital's delivery room. Thanks to CFD methods, it is possible to improve devices without any risk for infant.

The presented calculations and measurements show that the models properly describe physical phenomena in radiant warmers. The calculations give results which are consistent with intuition and experiment.

Time computations are also very important and they strongly depend on a number of elements in an analysed domain and on computers which were used during calculations. Computations take respectively 4 hours for 2D model and about 16 hours for the 3D model using eight-core processor. The reason of time differences between these two cases appears because, in 2D model, domain is limited to the volume next to the bed and a shape of infant is simpler than in 3D case. In fact, the natural large hospital room should be considered but it can take a huge number of elements. Of course near the walls, where velocity and temperature gradient is not too large, number of elements can be limited. However, next to the baby, because of occurring gradient, small elements are required. Finally, according to experimental room where validation will be made domain dimensions were reduced.

The $k-\varepsilon$ RNG turbulence model was chosen after comparison of the results of several turbulent models with experiments (which were not presented in the paper). In fact, the 2D model does not well describe turbulent phenomena because of the 3D nature of turbulence. This is the fact which distinguishes 2D and 3D results, so computations in these cases are not the same.

Discrepancies in value of human skin emissivity were the reason to carry out measurements. Temperature fields on more than eight healthy infants were checked. The results showed that skin emissivity is 0.95 and this value was used in the calculations.

All of the computations were calculated as steady-state cases. However, as it can be noticed, temperature field is not symmetrical on both sides of the model. This is a reason why in the future development these phenomena should be calculated as a transient.

The other reason why the results are not the same is the ones in 3D case is the fact that plastic shields were added, as it was mentioned in the previous section. This changed velocity and temperature fields in a domain.

In future work, a full model of thermoregulation in a human body will be introduced to the model.

Concluding, the presented numerical models are good base for future work with improving and reconstructing the infants' heating devices without any risk for infants.

ACKNOWLEDGEMENTS

The work has been financed by the Ministry of Science and Higher Education of Poland, Grant no N N512 477 039.

REFERENCES

- [1] www.atom-ami.co.jp, *online access February 2013*.
- [2] www.draeger-medical.com, *online access February 2013*.
- [3] www.neonatology.org, *online access February 2013*.
- [4] www.wikipedia.org, *online access February 2013*.
- [5] S. Arkell, P. Blair, J. Henderson. Is the mattress important in helping babies keep warm? Paradoxical effects of a sleeping surface with negligible thermal resistance. *Foundation Acta Paediatrica/Acta Paediatrica*, **96**: 199–205, 2007.
- [6] ASHRAE *Handbook: Fundamentals*. Physiological principles, comfort and health, 9–9, Atlanta, 1989.
- [7] Babytherm® 8004/8010 radiant warmer. Instruction for use. Dräger Medical AG & Co. KGaA.
- [8] M. Baumert. *Neonatology Classes*. Medical University of Silesia, Katowice, 2004 (in Polish).
- [9] E.F. Bell. *Infant incubators and radiant warmers*. Early human development, Department of Pediatrics, University of Iowa, Iowa City, Iowa, U.S.A., 1983.
- [10] E.F. Bell, G.R. Rios. A double-walled incubator alters the partition of body heat loss of premature infants. *Pediatr. Res.*, **17**: 135–140, 1983.
- [11] D.R. Bhatt, R. White, G. Martin, L.J. Van Marter, N. Finer, J.P. Goldsmith, C. Ramos, S. Kukreja, R. Ramanathan. Transitional hypothermia in preterm newborns. *Journal of Perinatology*, **27**: S45–S47, 2007.
- [12] C.J. Chen. *Fundamentals of turbulence modeling*. Taylor & Francis, 1998.
- [13] M. Chiswic. Commentary on current World Health Organization definitions used in perinatal statistics. *Archives of Disease in Childhood*, **61**(7): 708–710, 1986.
- [14] L. Douret, M. Robin, M.T. Le Normand. *Early child development and care*. Taylor & Francis, 2007.
- [15] *Fluent ANSYS in ANSYSs Workbench User's Guide* Realise 14.0, November 2011.
- [16] M.K. Ginalski. *Numerical analysis of heat and mass transfer processes within an infant incubator*. Institute of Thermal Technology, Silesian University of Technology, Gliwice, Poland, 2007.
- [17] T. Gomella. *Neonatology, Clinical Textbook*. Medical University of Silesia, Katowice, 1993 (in Polish).
- [18] P.S. Greer. Head Coverings for Newborns under Radiant Warmers. *Journal Obstetric Gynecology Neonatal Nursing* (JOGNN), **4**, 1988.
- [19] J. Koch. Transport incubator equipment. *Semi Neonatol*, **3**: 241–245, 1999.
- [20] E. Kostowski. *Heat Transfer Exercise Book*. Publishing House of the Silesian University of Technology, Gliwice, 2003 (in Polish).
- [21] P.A. Libby. *Introduction to turbulence*. Taylor & Francis, 1996.
- [22] J.H. Lienhard IV, J.H. Lienhard V. *A heat transfer textbook*. Phlogiston Press, Cambridge, Massachusetts U.S.A., version 1.31, January 16, 2008.
- [23] R.C. Lussky. *A century of neonatal medicine*. Minesota Medical Association, **82**: 1999.
- [24] A. Lyon. Applied physiology: Temperature control in the newborn infant. *Current Paediatrics*, **16**: 386–392, 2006.

-
- [25] M. Mazurak, M. Czyżewska. Incubator doctor and the Dionne quintuplets: on the phenomenon of Eexhibiting premature infants. *Dent. Med. Probl.*, **43**(2): 313–316, 2006.
- [26] A.C. Mellien. Incubator versus mothers’ arms: Body temperature conservation in very-low-bright-weight premature infants. *Jognn*, 2001.
- [27] W.J. Minkowycz, E.M. Sparrow, J.Y. Murthy. *Handbook of numerical heat transfer*. John Wiley & Sons, Inc., Haboken, New Jersey, 2006.
- [28] I. Norska-Borówka. *Diagnosis and Treatment of Newborns*. Medical University of Silesia, Katowice, 1994 (in Polish).
- [29] I. Norska-Borówka. *Alarming conditions in Newborns*. PZWL, Warszawa, 1993 (in Polish).
- [30] K. Parsons. *Human thermal environments*. Taylor & Francis, 2003.
- [31] A.E. Paterson. *A first course in fluid dynamics*. Cambridge University Press, 1983.
- [32] M. Radshaw, R. Rivers, D. Rosenblatt. *Born too early. Special care for your preterm baby*. Oxford University Press Inc., 1985.
- [33] S.A. Richards. *Temperature regulation*. Wykeham Publications (London) Ltd., 1973.
- [34] H.K. Silver, C.H. Kempe, H.B. Bruyn, V.A. Fulginiti. *Handbook of pediatrics*. Appleton & Lange, 1987.
- [35] J.K. Sweeney. *The high-risk neonate: developmental therapy perspectives*. The Haworth Press, Inc., 1986.
- [36] J. Szczapa. *Neonatology*. PZWL, Warszawa, 2001 (in Polish).
- [37] H.K. Versteeg, W. Malalasekera. *An introduction to computational fluid dynamics – THE FINITE VOLUME METHOD*. Pearson Education Limited, 2007.